

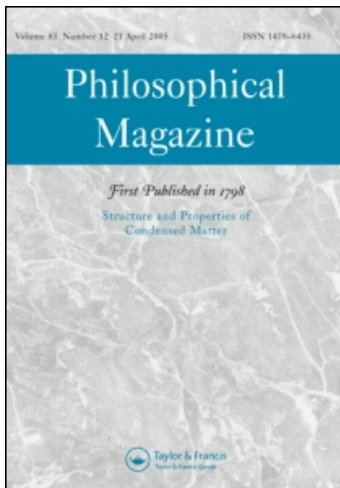
This article was downloaded by: [Giannattasio, Armando]

On: 5 August 2010

Access details: Access Details: [subscription number 924782143]

Publisher Taylor & Francis

Informa Ltd Registered in England and Wales Registered Number: 1072954 Registered office: Mortimer House, 37-41 Mortimer Street, London W1T 3JH, UK



Philosophical Magazine

Publication details, including instructions for authors and subscription information:
<http://www.informaworld.com/smpp/title~content=t713695589>

Brittle-ductile transitions in polycrystalline tungsten

A. Giannattasio^a; Z. Yao^a; E. Tarleton^a; S. G. Roberts^a

^a Department of Materials, University of Oxford, Oxford, OX1 3PH, UK

First published on: 27 July 2010

To cite this Article Giannattasio, A. , Yao, Z. , Tarleton, E. and Roberts, S. G.(2010) 'Brittle-ductile transitions in polycrystalline tungsten', Philosophical Magazine,, First published on: 27 July 2010 (iFirst)

To link to this Article: DOI: 10.1080/14786435.2010.502145

URL: <http://dx.doi.org/10.1080/14786435.2010.502145>

PLEASE SCROLL DOWN FOR ARTICLE

Full terms and conditions of use: <http://www.informaworld.com/terms-and-conditions-of-access.pdf>

This article may be used for research, teaching and private study purposes. Any substantial or systematic reproduction, re-distribution, re-selling, loan or sub-licensing, systematic supply or distribution in any form to anyone is expressly forbidden.

The publisher does not give any warranty express or implied or make any representation that the contents will be complete or accurate or up to date. The accuracy of any instructions, formulae and drug doses should be independently verified with primary sources. The publisher shall not be liable for any loss, actions, claims, proceedings, demand or costs or damages whatsoever or howsoever caused arising directly or indirectly in connection with or arising out of the use of this material.

Brittle–ductile transitions in polycrystalline tungsten

A. Giannattasio*, Z. Yao, E. Tarleton and S.G. Roberts

Department of Materials, University of Oxford, Parks Road, Oxford, OX1 3PH, UK

(Received 1 March 2010; final version received 14 June 2010)

The strain rate dependence of the brittle-to-ductile transition (BDT) temperature was investigated in notched and un-notched miniature bars made of high-purity polycrystalline tungsten and in notched bars of less-pure sintered material. The activation energy, E_{BDT} , for the process controlling the BDT in pure tungsten was equal to 1.0 eV both in un-notched and notched specimens, though the brittle–ductile transition temperature, T_{BDT} , was ≈ 40 K lower at each strain rate for the un-notched samples, indicating that the activation energy, E_{BDT} , is a materials parameter, independent of geometrical factors. The experimental data obtained from pure tungsten are described well by a two-dimensional dislocation-dynamics model of crack-tip plasticity, which is also discussed. For sintered tungsten, E_{BDT} was found to be 1.45 eV; T_{BDT} at a given strain rate was higher than in the pure tungsten by ≈ 90 K, suggesting that the BDT in tungsten is very sensitive to impurity levels.

Keywords: tungsten; fracture; dislocation; brittle–ductile transition; plasticity; purity

1. Introduction

Tungsten has been proposed as a plasma-facing material for critical components, subjected to high levels of radiation damage, high temperatures and stresses, in next-generation fusion reactors such as ITER [1]. At room temperature, tungsten generally fails by low-energy brittle cleavage; above a critical brittle–ductile transition temperature, T_{BDT} , the fracture mode may be ductile, with a greater or lesser amount of crack-tip or macroscopic plastic deformation [2]. One of the major concerns about tungsten being used for fusion applications is its high T_{BDT} . Brittle-to-ductile transition temperatures typically depend on strain rate, with T_{BDT} being lower at higher strain rates. Stresses produced at high loading rates by thermal/electromagnetic shock during a transient event (for example, a plasma disruption) are known to lead to formation of cracks in tungsten [3,4] and could possibly lead to catastrophic failure in practice. Also, in such applications, the transition temperature will also be lowered by radiation damage and helium accumulation, which are likely to decrease plasticity and to weaken grain boundaries.

There is thus a need to understand the mechanisms controlling the T_{BDT} and its strain-rate dependence in high purity tungsten and in commercial tungsten grades.

*Corresponding author. Email: agiannattasio@memc.it

Data on brittle-ductile transitions in tungsten are scarce and mostly related to pure crystals [2,5]. In studies of the brittle–ductile transition (BDT) in single-phase materials, such as silicon [6], germanium [7], alumina [8], T_{BDT} was measured as a function of strain rate, $\dot{\epsilon}$, and the following relationship was experimentally obtained:

$$\dot{\epsilon} = A \exp\left(-\frac{E_{\text{BDT}}}{kT_{\text{BDT}}}\right), \quad (1)$$

where A is a constant and k is Boltzmann’s constant. The activation energy for the BDT, E_{BDT} , was found to be equal to that experimentally found for dislocation glide [9]. This implies that the controlling process for the BDT in these materials is dislocation glide in the region near the crack-tip (rather than whether dislocations can be nucleated at or near the crack-tip). In these materials, dislocation-dynamics models of slip around crack-tips and the elastic ‘shielding’ of the crack-tip by the active dislocations can fit experimental results to high accuracy [10]. Similar modelling of the BDT in some bcc metals (Fe, V, Mo) has been performed with some success [11,12], but has been hampered by the lack of experimental data on dislocation velocity, which is difficult to measure in bcc metals using conventional etch-pitting techniques such as those successfully adopted for semiconductors (for example Si, Ge [12] and GaAs [13]).

In general, the expansion of dislocation loops from crack-tips in bcc metals requires motion of both screw dislocations and edge dislocations, but the dislocation nucleation rate in the general case will be controlled by the rate at which the slower screw dislocations can move away from crack-tip sources [14]. In a study of the BDT in single-crystal tungsten, Gumbsch et al. [5] deduced an activation energy for the BDT, E_{BDT} , of approximately 0.2 eV. This value is considerably lower than the activation energy required to promote glide of screw dislocations by nucleation of double-kinks (1.74 eV [15]); this may be attributed to the crystallographic orientation of the specimens used in the experiments reported in [5], which uniquely allows the controlling process to be the glide of edge dislocations [2]. In similar experiments using single-crystal specimens of a different orientation and fine-grained pure polycrystalline material, Giannattasio and Roberts deduced an activation energy of 1.05 eV, and attributed the difference between this activation energy and that for double-kink nucleation to the action of the shear stresses acting on dislocations in the array; this hypothesis was consistent with modelling of crack-tip plastic zones by 2D dislocation-dynamics [2,16,17].

This paper reports: (a) effects of impurities on the brittle–ductile transition in tungsten, comparing data from sintered commercial tungsten with those previously published for the same specimen configuration for pure polycrystalline tungsten [2]; (b) effects of specimen configuration on the brittle–ductile transition in pure tungsten, comparing un-notched with pre-cracked specimens.

2. Experimental details

The materials studied were 99.99% pure tungsten polycrystals (Metal Crystals and Oxides Ltd, Cambridge, UK) and commercial sintered tungsten, nominal purity

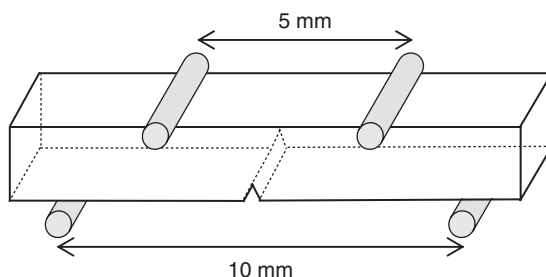


Figure 1. Geometry of the four-point bend tests on specimens of 1 mm \times 1 mm cross-section. The samples were loaded such that the notch and pre-crack were on the tensile face of the specimen.

99.97% (excluding Mo) (Plansee SE, Reutte, Austria). The sintered tungsten material was in two forms: as-sintered, and subjected to a post-sintering high temperature deformation treatment.

The nominal chemical composition of the sintered tungsten included Mo (100 appm), Fe (30 appm), C (30 appm), Cr, Ta, O, Si, P (all present at 20 appm), with other elements in concentration ≤ 10 appm. TEM investigation of the sintered/deformed material revealed the presence of thorium-containing particles in the matrix and also at grain boundaries, although the density of these visible particles (approximately 50 nm in size) was very low. Thorium was possibly introduced as an impurity during the mechanical deformation at high temperature, which was performed in the same furnaces and machines as those used to produce ‘thoriated’ tungsten (W containing 2% by weight of ThO₂), a material largely used in arc welding applications [18].

Brittle–ductile transition behaviour was investigated using four-point bend testing of bars with rectangular shape (1 mm \times 1 mm \times 11 mm), as shown in Figure 1. The small tungsten bars were cut using a circular saw with a diamond-coated blade and then were mechanically polished on three sides. Electropolishing at 10 V in 2 wt % NaOH solution was carried out to remove most of the residual damage from these surfaces. Electron backscattered diffraction (EBSD) was used to determine grain sizes: for the pure polycrystalline material the mean grain size was ≈ 3 μm , whereas sintered/deformed tungsten contained larger grains of size of ≈ 50 μm , although smaller sub-grains were also observed. Pre-cracks (~ 60 μm deep) were produced on the tensile faces of the test bars by using a sharp edge in a spark erosion machine for a few seconds at room temperature. Pre-cracks were a combination of a wedge notch and sharp thermally-induced pop-in cracks, which were found to be a mixture of intergranular and transgranular cracks with randomly distributed orientations.

Fracture tests were conducted in the temperature range 77–610 K. For temperatures above 300 K, the tests were carried out in a flowing argon gas atmosphere, whereas below room temperature they were conducted in a cooling nitrogen atmosphere. Specimens were tested at five outer-fibre strain rates in the range 4×10^{-5} – 5×10^{-2} s⁻¹ (at the specimen surfaces, the strain is proportional to the measured deflection; see [19] for details). For pre-cracked specimens this gives, dK/dt in the range 0.2–250 MPa m^{1/2} s⁻¹. Specimens which fractured with no plastic strain

(deduced from stress/strain curves) were considered to be fully brittle; those which did not fracture after >5% of plastic strain (the test rig's limit) were considered to be fully ductile; those which fractured in an apparently brittle manner after a limited amount of plastic strain were designated as 'semi-brittle'. Further details of the fracture surfaces and plastic strain observed in pure tungsten bars can be found elsewhere [2].

Pure polycrystalline tungsten bars, which did not have any intentional notch/pre-crack, were also prepared and tested under the same conditions as the notched samples in order to investigate possible influences of specimen geometry or test configuration on T_{BDT} and E_{BDT} .

3. Results

Figure 2 shows the measured fracture toughness, $K_{\text{Ic}} = \sigma_F \sqrt{\pi c}$ (where σ_F is the fracture stress and c is the total crack depth as measured on each specimen), as a function of temperature and strain rate for sintered tungsten, and (from [2], for comparison) similar results for pure single-crystal and polycrystalline tungsten. For ductile specimens which did not fail by brittle or semi-brittle cleavage, the stress intensity factor at yield, $K_{\text{Iy}} = \sigma_y \sqrt{\pi c}$, (where σ_y is the measured yield stress) is plotted. The purely brittle fracture toughness measure at 77 K was $4.6 \pm 0.3 \text{ MPa m}^{1/2}$ in pure polycrystalline and $5.4 \pm 0.9 \text{ MPa m}^{1/2}$ in sintered and deformed tungsten. These low temperature results are in agreement with data from previous investigations of the BDT in polycrystalline tungsten by other authors [20] but are higher than those found in single-crystal tungsten ($2.7 \pm 0.2 \text{ MPa m}^{1/2}$) [2,5] where fast fracture occurs easily on the low energy {100} cleavage planes. In these polycrystalline materials, fracture was by transgranular cleavage ('pure' and 'sintered and deformed') and approximately 70:30 transgranular cleavage:intergranular fracture ('sintered').

With increasing temperature, the fracture toughness increased steadily in all the materials, though final failure was still by rapid brittle fracture (i.e. 'semi-brittle' behaviour). Over the whole semi-brittle range, the fracture toughness of pure polycrystalline tungsten was larger than that of the sintered tungsten. This is possibly due to its smaller grain size.

Above a critical temperature, pure tungsten and sintered/deformed tungsten specimens no longer fractured but bent in a ductile manner, up to the strain limit possible in the test jig. For each value of the strain rate, the transition from semi-brittle to fully ductile behaviour occurred over a very narrow temperature range. The transition temperature, T_{BDT} , for these materials increased with increasing strain rate.

The as-sintered material fractured in a brittle manner at all temperatures up to 800°C, the limit of the test apparatus. This may be due to grain-boundary embrittlement by impurity segregation, combined with some residual porosity from the sintering process. Such behaviour correlates with high-temperature brittleness observed in thermal shock experiments performed using similarly sintered tungsten [3,4].

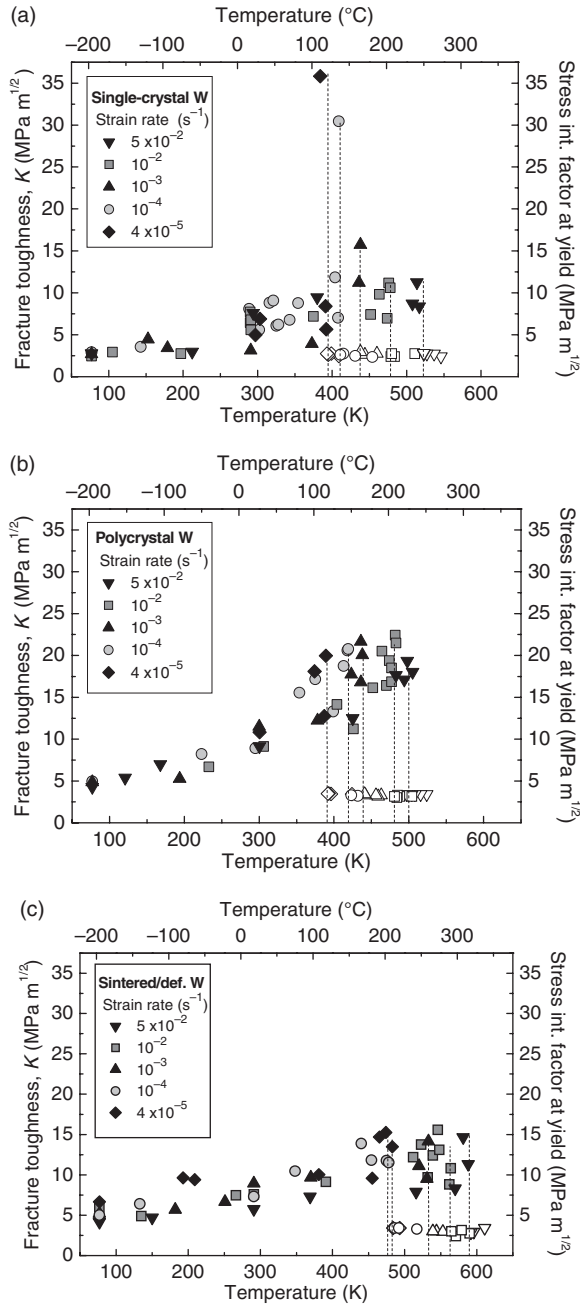


Figure 2. Fracture toughness (solid symbols, left axis) measured in pure tungsten ((a) polycrystal [2] and (b) single-crystals [2]) and (c) in sintered/deformed tungsten materials as a function of temperature and strain rate. Open symbols represent ductile specimens (no fracture events, right axis). The vertical dotted lines mark the brittle–ductile transition at each strain rate. Taken from *Strain-rate of the brittle-to-ductile transition temperature in tungsten*, A. Giannattasio and S.G. Roberts, *Philosophical Magazine A*, Vol. 87, Issue 17, 2007, reprinted by permission of Taylor & Francis Ltd. <http://www.tandf.co.uk/journals>.

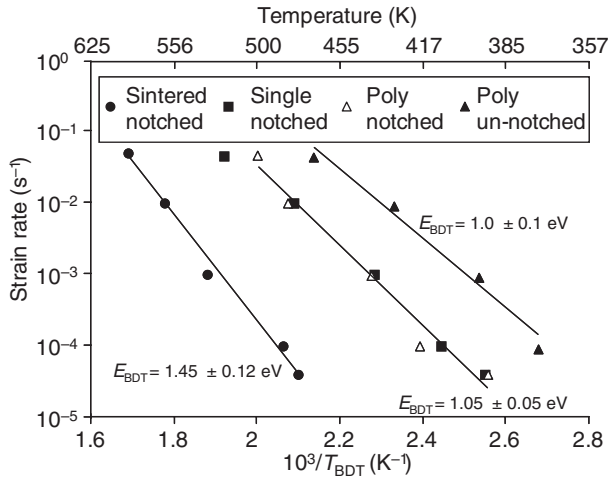


Figure 3. Arrhenius plot of the strain rate versus reciprocal T_{BDT} for the different tungsten materials investigated. Data obtained from un-notched pure polycrystalline samples are also shown.

3.1. Activation energies for the BDT

Figure 3 shows an Arrhenius plot of the measured T_{BDT} as a function of strain rate for the materials that exhibited a brittle–ductile transition; data from notched single-crystal tungsten [2] are also shown for comparison. The slope of the straight lines in the plot gives activation energies, E_{BDT} , via Equation (1).

Sintered and deformed tungsten is more brittle than the pure materials; T_{BDT} is ~ 80 K higher for all the strain rates used. Intergranular fracture was not observed in this material, implying that the effects of any impurities on the fracture process are via modification of the behaviour of the ‘bulk’ materials, rather than by segregation to, and weakening of, grain boundaries. The value of E_{BDT} derived for sintered and deformed tungsten is 1.45 eV, higher than that for pure tungsten (1.05 eV). This indicates that dislocations have to overcome a higher energy barrier in order to glide, probably because of interaction with solute atoms. The difference observed in activation energies between pure and sintered tungsten is consistent with typical values of the binding energy of a solute atom to a dislocation: ~ 0.2 – 0.5 eV in metals [21].

In high-purity tungsten, the value of E_{BDT} is independent of the presence of grains or pre-cracks in the crystal, being $E_{BDT} \approx 1.05$ eV in both single-crystal and notched and un-notched polycrystalline material. In un-notched pure tungsten bars, the absence of a pre-crack in the specimens induces a downwards shift in T_{BDT} of approximately 40 K (i.e. such specimens are more ductile, as would be expected given the absence of a pre-crack), but the activation energy is unchanged. This indicates that the basic process controlling the brittle–ductile transition is the same in all the pure tungsten materials, independent of details of the test specimen geometry. This process has been identified [2] as the glide of dislocations from near-crack-tip sources and the influence of these dislocations on the crack-tip stress field

(‘dislocation shielding’). The values of the brittle–ductile transition temperature, T_{BDT} , in pre-cracked specimens are the same for pure single-crystal and polycrystalline tungsten; the implication is that dislocation motion near the crack-tip is not significantly affected by the presence of grain boundaries.

4. Modelling

4.1. Dislocation dynamics model for the BDT

A simple two-dimensional discrete dislocation-dynamics model for crack-tip plasticity [22,23] has been developed further to predict the variation of semi-brittle fracture toughness with temperature and brittle-ductile transition temperatures for body-centred cubic metals [16,17]. The model differs from earlier versions (such as [22]) in that dislocations are nucleated and glide on two slip planes orientated symmetrically above and below the crack plane, rather than only one slip plane. In each cycle of the model, occupying a small time-step, the stress on each dislocation, τ_i , at a position along the slip plane r_i is calculated using

$$\tau_i = \frac{K_{\text{app}}}{r_i^{1/2}} F(\theta) + \frac{K_{\text{app}}}{c^{1/2}} G(r_i, \theta, c, L) + \frac{\mu}{r_i} H(\theta) + \mu \sum_{j \neq i} M((r_i - r_j)^{-1}, \theta). \quad (2)$$

The first term represents stresses from the crack-tip field; the second term represents bend stresses and the third term represents interaction stresses arising from image dislocations (present because of the free surfaces at the crack). The final term accounts for interaction stresses between the dislocations (both between dislocations on the same slip plane, and between the two slip planes). Explicit expressions for the first, third and fourth terms can be found in [24] and the second term is a linear bending term for the experiments being modelled here having the form $G \propto 1 - 2r_i \cos \theta / L$. The other parameters are taken from the experiments being modelled. K_{app} is the applied stress intensity factor, which is proportional to the applied strain. θ is the inclination of the slip plane to the crack (45° for $\{110\}$ slip planes in the single-crystal beam with all sides aligned along $\{100\}$), c is the pre-crack length ($60 \mu\text{m}$), L is the specimen thickness (1 mm) and μ is the shear modulus of tungsten, (161 GPa). The Burgers vector magnitude, b , was taken as 0.274 nm (see Figure 4).

If the net stress at the dislocation, source position (placed at $r = 30b$) is positive, then a new dislocation is nucleated at each of the symmetric sources above and below the crack-tip. Dislocations are moved over a small time-step, according to a screw dislocation velocity law based on the nucleation of kink pairs [25,26]:

$$v_i = v_0 \exp\left(\frac{-E_{kp}(\tau_i)}{K_B T}\right), \quad E_{kp}(\tau) = 2H_{kp} - 2\alpha\tau_i^{1/2}, \quad (3)$$

where $2H_{kp}$ is the energy required to nucleate a kink pair at zero stress (1.75 eV [15]) and the stress on each dislocation is calculated using Equation (2). The parameter 2α appearing in Equation (3) is defined by

$$2\alpha = (2a^3 b \gamma_0)^{1/2} = 6.8 \times 10^{-24} \text{ m}^2 \text{ N}^{1/2}. \quad (4)$$

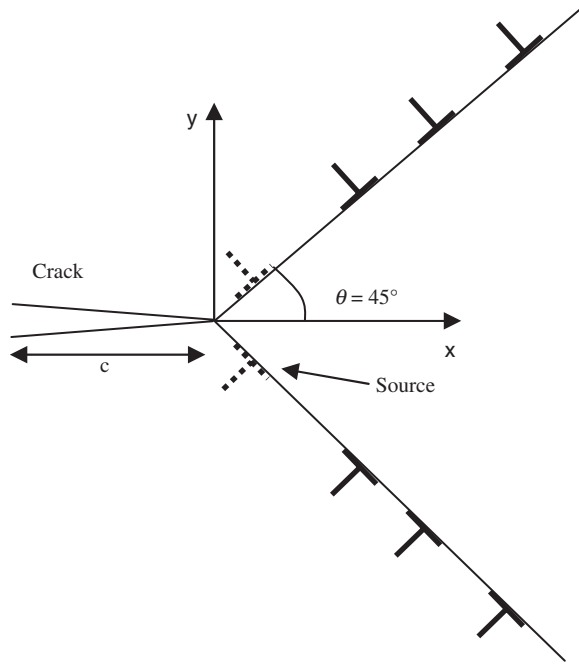


Figure 4. Schematic of the model. Dislocations are nucleated near the crack-tip when the local stress is positive, and glide on the slip planes at 45° to the crack plane. The dislocations influence the crack-tip stress field via elastic shielding. See text for details.

The numerical values of the parameters used in Equation (4) were obtained experimentally for tungsten by Brunner and Glebovsky [27]: a is the kink height (4.459×10^{-10} m), b is the Burgers vector magnitude (2.74×10^{-10} m) and γ_0 is the pre-logarithmic factor of the line tension (9.55×10^{-10} N). The only unknown parameter in the model is the velocity law pre-factor, v_0 , appearing in Equation (3); the value of this was fixed by fitting the predicted transition temperature, T_{BDT} , to experimental data for the lowest strain rate used for each material type modelled (see Section 4.3).

The stress intensity at the crack-tip, K_{tip} , which is lower than the applied value K_{app} due to dislocation shielding, is calculated using

$$K_{\text{tip}}(t) = K_{\text{app}}(t) - K_{\text{dis}}(t) = \dot{K}_{\text{app}}t - \frac{\mu f(\theta)}{\sqrt{2\pi(1-\nu)}} \sum_{i=1}^{N(t)} \frac{1}{\sqrt{r_i(t)}}, \quad (5)$$

where the applied loading rate $\dot{K}_{\text{app}} \propto \dot{\epsilon}$, and $f(\theta)$ is as given in [24]. The dynamic part of the dislocation shielding term depends only on the distance of each dislocation from the crack-tip, $r_i(t)$, and the number of dislocations, $N(t)$. The shielding term, $K_{\text{dis}}(t)$, was found in the model to increase non-linearly in time, whereas $K_{\text{app}}(t)$ increases linearly. At high temperatures where dislocations are readily emitted from crack-tip sources, the effects of shielding can be strong enough after some time t_m that $\dot{K}_{\text{app}}(t_m) = \dot{K}_{\text{dis}}(t_m)$, so that $\dot{K}_{\text{tip}}(t_m) = 0$. K_{tip} then has a maximum value at t_m

and if $K_{tip}(t_m)$ is below the critical value for cleavage fracture K_{Ic} (2 MPa m^{1/2} for tungsten [28]), then K_{Ic} will never be reached and ductile behaviour is predicted. At lower temperatures, fewer dislocations are emitted, so that the effects of shielding are weaker. K_{tip} can then reach the critical value for cleavage K_{Ic} , and fracture may occur, though at an elevated value of K_{app} , due to the effects of dislocation shielding. To model the BDT, the velocity law pre-factor v_0 in Equation (3) was chosen so that the modelled peak in K_{tip} occurred just below K_{Ic} at one strain rate (the lowest used experimentally) and at the corresponding transition temperature at that strain rate (see Section 4.3). Other strain rates were then simulated using this value of v_0 . The model was then found to produce a good fit to the change in transition temperature with strain rate in pure single-crystal tungsten; see [17] for details.

4.2. The velocity law pre-factor

The velocity law pre-factor for pure tungsten was set at 5.5×10^7 m s⁻¹ by fitting the transition temperature predicted by the model to the experimental value (392 K) at the slowest strain rate ($\dot{\epsilon} = 4 \times 10^{-5}$ s⁻¹). The velocity law pre-factor can also be estimated using the kink-pair model proposed by Seeger [25,26]:

$$v_0 \approx aN_dL_d \frac{2\pi H_{kp}}{\omega^2 \sqrt{\pi m_k k T}} \frac{1}{N_d} \approx \frac{3 \times 10^{17}}{N_d} \text{ (m s}^{-1}\text{)}, \quad (6)$$

where N_d is the dislocation density, L_d is the distance along the dislocation lines between obstacles that are insurmountable for the kinks (and the product $N_dL_d \approx 1.66 \times 10^5$ m⁻¹), m_k is the kink mass (1.69×10^{-26} kg) and w_k is the kink width (34.4×10^{-10} m). Values of the other parameters are given in [26]; those used were for a temperature characteristic of the experiments modelled (450 K). The velocity law pre-factor used in these simulations then implies a dislocation density of 5×10^9 m⁻², which is not unreasonable for a well-annealed pure metal.

It is possible to write the exponent in the velocity law, Equation (3), in the form

$$E_{kp}(\tau_i) = 2H_{kp} - 2\alpha\tau_i^{1/2} = 2H_{kp} - \tau_i V_A, \quad (7)$$

as has been done elsewhere [16,17]. This is consistent with the Seeger model [25] as the activation volume V_A in Equation (7) can be equated to $2V_{kp}$ where V_{kp} is the activation volume of kink-pair formation, defined in Seeger's model to be:

$$V_a = 2V_{kp} = -2 \left(\frac{\partial E_{kp}}{\partial \tau} \right)_{T=const} = \frac{2\alpha}{\sqrt{\tau}} \approx \frac{6.8 \times 10^{-24}}{\sqrt{\tau}} \text{ m}^3. \quad (8)$$

We have used the value of $\alpha = 3.4 \times 10^{-24}$ J for tungsten obtained by Brunner [26]. The stress in the simulated dislocation arrays was found to be approximately 300 MPa over the range of temperatures and strain rates modelled. Equation (8) then gives an activation volume V_A of $\approx 19b^3$; this in good agreement with the values used in the modelling [16,17] and with experimental measurements [27]. The dislocation velocity law used thus appears to be self-consistent, and in agreement with experimentally-measured parameters, where available.

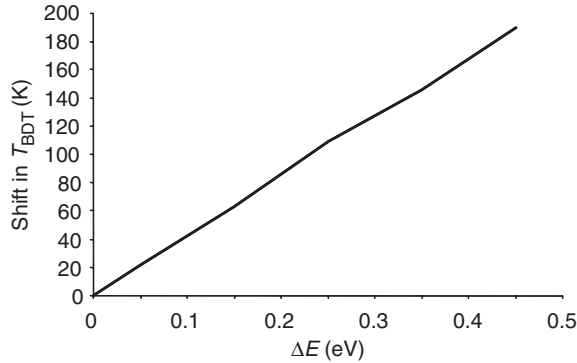


Figure 5. Modelling results: upward shift in the brittle–ductile transition temperature (at a strain rate of $4.0 \times 10^{-5} \text{ s}^{-1}$) resulting from increasing the kink-pair separation energy $E_{kp}(\tau)$ by an amount ΔE .

4.3. Modelling the effects of impurities on the BDT

To model the influence of impurities, the double-kink activation energy used in the dislocation mobility law was increased by an amount ΔE . The predicted transition temperature at a given strain rate was then found to increase linearly with the increase in activation energy (see Figure 5). The experimentally measured increase in T_{BDT} was approximately 90 K. To achieve this in the simulations a value of $\Delta E \approx 0.2 \text{ eV}$ is required. However, the experimentally found value of ΔE is $\approx 0.45 \text{ eV}$ (see Section 3.1). This may be because the 2D modelling used here can only introduce the influence of impurities on the dislocation mobility as an averaged effect, whereas in reality solutes atoms are more likely to act as local pinning centres distributed along the dislocation line. The model does not currently include the influence of grain boundaries so implicitly assumes that: (a) fracture is transgranular cleavage rather than intergranular (as is experimentally found for the material modelled); (b) grain boundaries do not exert a controlling influence on dislocation mobility (as is supported by the identity of activation energies and BDT temperatures for single-crystal and pure polycrystalline tungsten [2]).

4.4. Modelling the effect of crack size on the BDT

To model the BDT in specimens of pure tungsten without deliberately introduced notches, simulations were performed using a range of crack sizes between $60 \mu\text{m}$ (the crack sizes in intentionally notched samples [17]) and $10 \mu\text{m}$. The results are shown in Figure 6 and Table 1. The predicted T_{BDT} decreases with decreasing crack size. This reduction in T_{BDT} occurs because decreasing the crack size at a given strain rate decreases the applied stress intensity loading rate. The shift in T_{BDT} is larger at higher strain rates, being -55 K at $4.6 \times 10^{-2} \text{ s}^{-1}$ and -40 K at $4 \times 10^{-5} \text{ s}^{-1}$ for a $40 \mu\text{m}$ crack compared to a $60 \mu\text{m}$ crack. The experimentally observed shift in T_{BDT} between polycrystalline specimens with a notch and pre-crack $60 \mu\text{m}$ deep and un-notched polycrystalline specimens is of this order, implying that the size of the

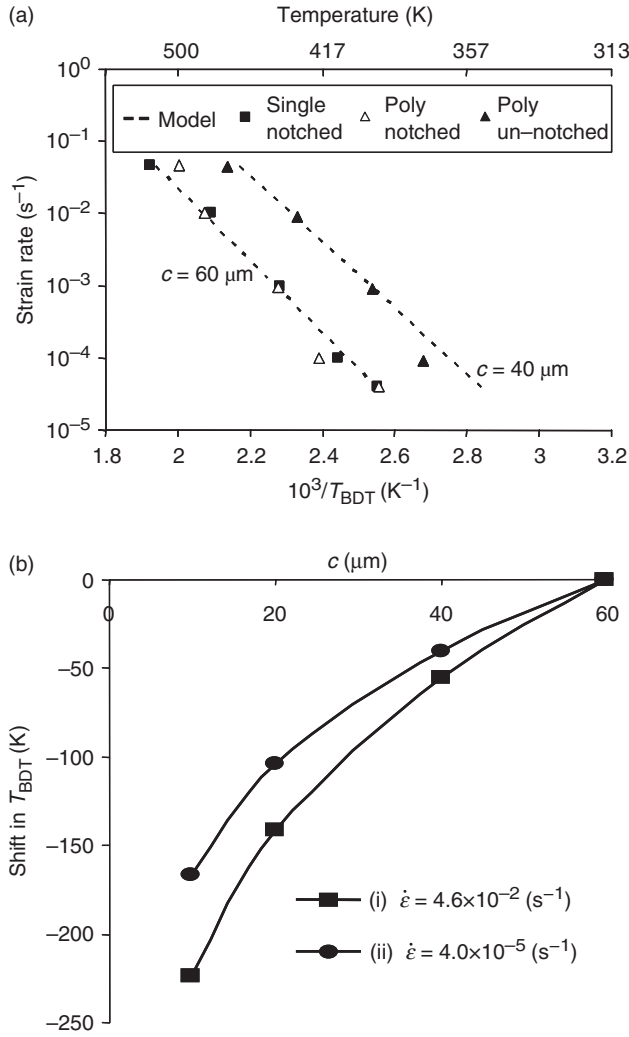


Figure 6. Modelling results: reducing the crack length gives a downward shift in T_{BDT} : (a) the predicted T_{BDT} for $c = 60 \mu m$ and $c = 40 \mu m$; also shown are the experimental data for the notched and un-notched bars. The predicted shifts in T_{BDT} for various crack sizes are shown in (b) for the fastest (i) and slowest (ii) strain rates.

Table 1. Predicted T_{BDT} (K) at the slowest ($4.0 \times 10^{-5} s^{-1}$) and fastest ($4.6 \times 10^{-2} s^{-1}$) strain rates for different simulated crack sizes. The experimental values for the notched sample were 392 K and 520 K.

c (μm)	60	40	20	10
$\dot{\epsilon} = 4.0 \times 10^{-5} s^{-1}$	$T_{BDT} = 392$ K	352 K	288 K	225 K
$\dot{\epsilon} = 4.6 \times 10^{-2} s^{-1}$	$T_{BDT} = 515$ K	460 K	374 K	291 K

critical flaws for fracture inherent in the microstructure of the polycrystalline material is $\approx 40 \mu\text{m}$.

5. Conclusions

The brittle–ductile transition (BDT) temperature as a function of strain rate has been measured in pure single- and polycrystalline tungsten bars and in commercial sintered and sintered + deformed material. In pure tungsten, the activation energy for the brittle–ductile transition, E_{BDT} , was found to be 1.05 eV, and did not change with specimen geometry (notched as compared to un-notched specimens) or with the presence of grain boundaries (polycrystalline as compared to single-crystal material). As-sintered tungsten showed brittle behaviour even at very high temperatures (800°C) and at low strain rates; this is most probably due to grain-boundary segregation of impurities, principally Mo, Fe and C, but possibly also Th). Thus its brittle–ductile transition behaviour could not be measured in these experiments. Sintered and deformed tungsten, containing the same impurities, but homogenised by the hot-working process, had higher BDT temperatures and a higher activation energy for the BDT (1.45 eV) than the pure materials.

The BDT temperature, T_{BDT} , even if measured at a fixed strain rate, cannot be considered as a physical constant characteristic of the material because T_{BDT} depends in general on sample geometry. The T_{BDT} temperatures themselves reported in this work are valid only for the specimen shape and size used here (rectangular bars with 1 mm^2 cross-section, tested in four-point bending), and are not necessarily applicable to other specimen or test types. However, the results presented here show that such geometrical factors do not affect the activation energy E_{BDT} of the BDT in tungsten, and hence its strain-rate dependence; this is specific to the material.

Dislocation-dynamics modelling of crack-tip dislocation behaviour was conducted. The model used a velocity law based on stress-assisted kink-pair nucleation. The parameters used in the model were found to be self-consistent and in agreement with experimental data. The modelled dislocation behaviour produces an explicit BDT when the simulated temperature is high enough for high enough rates of dislocation emission from the crack-tip for shielding to keep the crack-tip stress-intensity factor always below the cleavage value. The model could reproduce the experimentally found reduction in BDT temperatures with a reduction in crack length, and predicts a linear increase in transition temperature with increasing activation energy.

Acknowledgements

The authors thank Dr Sergio Lozano-Perez for help with TEM analysis. Support by UKAEA Culham laboratory and the EU project “ExtreMat”, contract NMP-CT-2004-500253, is gratefully acknowledged.

References

- [1] H. Bolt, V. Barabash, W. Krauss, J. Linke, R. Neu, S. Suzuki and N. Yoshida, *J. Nucl. Mater.* 329 (2004) p.66.

- [2] A. Giannattasio and S.G. Roberts, *Phil. Mag.* A 87 (2007) p.2589.
- [3] V.A. Makhlay, A.N. Bandura, O.V. Byrka, I.E. Garkusha, V.V. Chebotarev, V.I. Tereshin and I. Landman, *Phys. Scripta* T128 (2007) p.239.
- [4] T. Hirai, E. Bondarchuk, A.I. Borovkov, T. Koppitz, J. Linke, P. Mertens, O. Neubauer, A. Panin, V. Philipps, G. Pintsuk, S. Sadakov, R.W. Steinbrech, B. Schweer, I. Uytendhouwen, R. Vaen, U. Samm and R. Sievering, *Phys. Scripta* T128 (2007) p.144.
- [5] P. Gumbsch, J. Riedle, A. Hartmaier and H.F. Fischmeister, *Science* 282 (1998) p.1293.
- [6] S.G. Roberts and J. Samuels, *Proc. Roy. Soc. Lond. Math. Phys. Sci.* 421 (1989) p.1.
- [7] F.C. Serbena and S.G. Roberts, *Acta Metall. Mater.* 42 (1994) p.2505.
- [8] S.G. Roberts, H.S. Kim and P.B. Hirsch, in *Proceeding of the 9th International Conference on the Strength of Metals and Alloys, Haifa, July 1991*, D.G. Brandon, R. Chaim and A. Rosen, eds., Freund, London, 1991, p.783.
- [9] M. Brede and P. Haasen, *Acta Metall.* 36 (1988) p.2003.
- [10] P.B. Hirsch and S.G. Roberts, *Phil. Trans. Roy. Soc. Lond. A* 355 (1997) p.1991.
- [11] P.B. Hirsch, A.S. Booth, M. Ellis and S.G. Roberts, *Scripta Metall. Mater.* 27 (1992) p.1723.
- [12] A. Giannattasio, M. Tanaka, T.D. Joseph and S.G. Roberts, *Phys. Scripta* T128 (2007) p.87.
- [13] S. Fujita, K. Maeda and S. Hyodo, *Phil. Mag.* 65 (1992) p.13.
- [14] B.W. Lagow, I.M. Robertson, M. Jouiad, D.H. Lassila, T.C. Lee and H.K. Birnbaum, *Mater. Sci. Eng. A* 309–310 (2001) p.445.
- [15] D. Brunner, *Mater. Trans. JIM* 41 (2000) p.152.
- [16] M. Tanaka, E. Tarleton and S.G. Roberts, *Acta. Mater.* 56 (2008) p.5123.
- [17] E. Tarleton and S.G. Roberts, *Phil. Mag.* 89 (2009) p.1478.
- [18] I. Langmuir, *Phys. Rev.* 22 (1923) p.357.
- [19] P. Ponraj and S. Ramakrishnaiyer, *J. Mater. Sci. Lett.* 11 (1992) p.1000.
- [20] P. Gumbsch, *J. Nucl. Mater.* 323 (2003) p.304.
- [21] D. Hall and D.J. Bacon, *Introduction to Dislocations*, Butterworth-Heinemann, Oxford, 2001.
- [22] P.B. Hirsch, S.G. Roberts and J. Samuels, *Scripta Metall.* 21 (1987) p.1523.
- [23] S.G. Roberts, S.J. Noronha, A.J. Wilkinson and P.B. Hirsch, *Acta Mater.* 50 (2002) p.1229.
- [24] V. Lakshmanan and J.C.M. Li, *Mater. Sci. Eng. A* 104 (1988) p.95.
- [25] F. Ackermann, H. Mughrabi and A. Seeger, *Acta Metall.* 31 (1983) p.1353.
- [26] D. Brunner, *Mater. Trans. JIM* 41 (2000) p.152.
- [27] D. Brunner and V. Glebovsky, *Mater. Lett.* 44 (2000) p.144.
- [28] L. Vitos, A.V. Ruban, H.L. Skriver and J. Kollar, *Surf. Sci.* 411 (1998) p.186.